



Controlling energy deposition during the C_{60}^+ bombardment of silicon: The effect of incident angle geometry

Joseph Kozole*, Nicholas Winograd

Department of Chemistry, Penn State University, University Park, PA 16802, USA

ARTICLE INFO

Article history:

Available online 18 May 2008

Keywords:

SIMS
 C_{60}^+
 Silicon
 Depth profiling

ABSTRACT

The profile of the energy deposition footprint is controlled during the C_{60}^+ erosion of Si surfaces by varying the incident energy and/or incident angle geometry. Sputter yield, surface topography, and chemical composition of the eroded surfaces were characterized using atomic force microscopy (AFM) and secondary ion mass spectrometry (SIMS). The experiments show that the 10 keV, 40° incident C_{60}^+ erosion of Si results in the formation of a C containing, mound-like structure on the solid surface. We find that the occurrence of this C feature can be avoided by increasing the incident energy of the C_{60}^+ projectile or by increasing the incident angle of the C_{60}^+ projectile. While both strategies allow for the Si samples to be eroded, the occurrence of topographical roughening limits the usefulness of C_{60}^+ in ultra-high resolution semiconductor depth profiling. Moreover, we find that the relative effect of changing the incident angle geometry of the C_{60}^+ projectile on the profile of the energy deposition footprint, and thus the sputter yield, changes according to the kinetic energy of the projectile and the material of the bombarded surface, a behavior that is quite different than what is observed for an atomic counterpart.

© 2008 Elsevier B.V. All rights reserved.

1. Introduction

Atomic primary ion beams, such as Cs^+ , are routinely used for semiconductor depth profiling in secondary ion mass spectrometry (SIMS) [1]. For the experiments, the effect of incident energy and incident angle on the quality of the data obtained is well established [1,2]. Typically, a depth profile with 1 nm depth resolution can be acquired using a low energy (≤ 1 keV), glancing incidence ($\geq 50^\circ$ with respect to sample normal) ion beam [1,2].

The emergence of cluster primary ion beams, such as C_{60}^+ , has provided an alternative approach to SIMS depth profiling [3]. Because each C atom in a C_{60}^+ projectile carries 1/60th of the total energy, the depth at which the energy is deposited into the solid is substantially smaller than an atomic counterpart [4]. Since the depth resolution of the experiment is directly related to the altered depth, C_{60}^+ is a promising projectile for obtaining ultra-high depth resolution (≤ 1 nm) during erosion experiments.

To date, the application of C_{60}^+ to semiconductor depth profiling has been restricted by the occurrence of artifacts when Si is bombarded with C_{60}^+ [5]. The artifacts, which include the deposition of a C layer and the formation of topographical features,

severely limit, and in some cases eliminate, the ability of C_{60}^+ to erode the Si solid. Investigations have shown that the undesired effects can be minimized by increasing the incident energy of the C_{60}^+ to 15 keV or higher [5,6]. However, increasing the kinetic energy of the projectile decreases the depth resolution of the experiment [1,2,5].

The effect of changing the incident angle of the C_{60}^+ on the erosion of Si has yet to be examined. Molecular dynamics (MDs) simulations suggest the C_{60}^+ incident geometry is critical to the location at which the energy is deposited into a solid, a factor important in the determination of sputter yield and altered depth [6–8]. Additionally, a study on the effect of C_{60}^+ incident angle on the bombardment of a molecular solid finds that sputter yield does not increase with a $1/\cos \theta$ relationship, a behavior quite different than what is observed for atomic projectiles [9,10].

The objective of this research is to determine if the unique energy deposition process observed during C_{60}^+ bombardment can be manipulated in a way that the formation of artifacts during the erosion of Si is avoided and the prospect for performing ultra-high resolution semiconductor depth profiling is retained. Here, we report that the choice of incident energy and incident angle of the C_{60}^+ projectile strongly influences the Si sputtering yield, the C deposition probability, and the formation of topography. The results show that the 10 keV, 40° incident C_{60}^+ erosion of Si is limited by the deposition of a C layer and that the artifact can be

* Corresponding author.

E-mail address: jjk302@psu.edu (J. Kozole).

avoided by increasing the C_{60}^+ incident energy to 20 keV. At glancing incident angles, we find that C deposition is not observed at any of the examined incident energies. At this stage of the investigation, topographical roughening of the bombarded Si surface is found to be almost independent of erosion parameters, ranging from values of 4.4–5.9 nm, limiting the usefulness of C_{60}^+ in ultra-shallow depth profiling. We conclude with a discussion concerning the influence of incident geometry on the C_{60}^+ bombardment event.

2. Experimental

Sample analysis was performed using a ToF-SIMS instrument described previously [11]. A C_{60}^+ ion beam system (IOG-40, Ionoptika Ltd.) is mounted onto the instrument at a 40° angle with respect to sample normal [12]. The C_{60}^+ incident energies are varied from 10 keV to 120 keV. Higher C_{60}^+ energies are achieved by extracting the ions at 40 keV and selecting the C_{60}^{2+} and C_{60}^{3+} ions with a Wien filter. Under typical conditions, the C_{60}^+ ion beam current is 200 pA with a 5- μm ion beam size. The C_{60}^+ incident angle is varied using a customized sample target to adjust the sample tilt in reference to the ion beam. The C_{60}^+ incident angles used here are 40° and 75° .

Crystalline Si substrates (Ted Pella, Inc.) were sonicated in a 50/50% hexane/methanol mixture for 1 h, dried under a stream of N_2 gas, and introduced into a ToF-SIMS instrument. The Si samples were bombarded at a $\sim 200 \mu\text{m} \times 200 \mu\text{m}$ field of view and to a fluence of $\sim 2 \times 10^{16}$ C_{60}^+ ions per cm^2 . The chemical composition of the bombarded surface was characterized using SIMS. Chemical-specific SIMS images were acquired at a $400 \mu\text{m} \times 400 \mu\text{m}$ field of view using a focused 40 keV, 40° incident C_{60}^+ ion beam. The sputter yield and surface topography of the bombarded surface were measured using atomic force microscopy (AFM, Nanopics 2100, TLA Tencor, Inc.).

3. Results and discussion

To determine the prospect for performing ultra-high resolution semiconductor depth profiling using C_{60}^+ , sputter yield measurements from a Si solid were made using 10–120 keV C_{60}^+ incident energies at 40° and 75° C_{60}^+ incident angles. The yields were calculated using AFM to determine the volume removed from a Si crystal bombarded to a fluence of $\sim 2.0 \times 10^{16}$ C_{60}^+ per cm^2 . The yield measurements are reported in Fig. 1 while the corresponding crater shapes and SIMS images are shown in Fig. 2. For the 40 keV, 40° incident C_{60}^+ case illustrated in Fig. 2b, 4.15×10^{12} C_{60}^+ ions were used to remove 8.29×10^{14} Si atoms, corresponding to a yield of 200. The number of Si atoms was determined from the bombarded area of $150 \mu\text{m} \times 125 \mu\text{m}$, the bombarded depth of 885 nm, and the Si atomic density of 5.0×10^{22} molecules/ cm^3 . For the 40° incident geometry, the yield increases rapidly from 2 Si atoms at 10 keV impact energy to 200 atoms at 40 keV before reaching 300 atoms at 120 keV. For the 75° incident geometry, the yield increases linearly from 43 Si atoms at 10 keV impact energy to 200 atoms at 40 keV.

The yield trends in Fig. 1 identify several interesting points regarding the C_{60}^+ bombardment of Si. First, 10 keV, 40° incident C_{60}^+ is the only condition found where the Si sputter yield is exceedingly small. Second, when the C_{60}^+ incident energy is increased from 10 keV to 40 keV at 40° incidence, the yield increases by a factor of 100. Last, the yield at 10 keV, 40° incident C_{60}^+ is increased by a factor of 20 when the incident angle is increased to 75° . Collectively, the observations provide important insight into how the profile of the energy deposition footprint effects the formation of artifacts during the C_{60}^+ erosion of Si.

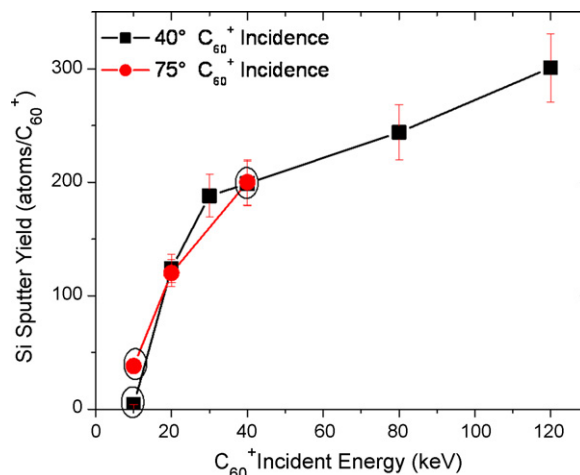


Fig. 1. Silicon sputter yield as a function of C_{60}^+ incident energy. The black squares represent the yield at 40° incidence and the red circles represent the yield at 75° incidence. The experimental error is $\pm 10\%$. The yields were calculated using AFM to determine the volume removed from a Si crystal bombarded to a fluence of $\sim 2.0 \times 10^{16}$ C_{60}^+ per cm^2 . The data for the points circled are shown in detail in Fig. 2a–c.

A summary of the 10 keV, 40° incident C_{60}^+ experiment is shown in Fig. 2a. The AFM representation and the AFM line profile of the bombarded Si surface show a mound-like structure within a shallow sputter crater. The SIMS images indicate that this mound consists of C only while the area surrounding the mound within the crater consists of a Si and C mixture. The observations support earlier experiments that describe 10 keV C_{60}^+ sputtering of Si by a transient period of net erosion followed by a period of net deposition [5]. This transition from erosion to deposition is explained by a C_{60}^+ fluence dependent change in the chemistry of the bombarded surface. The chemical change is attributed to the number of C atoms deposited into the Si being larger than the number of C atoms removed from the surface during C_{60}^+ erosion [13]. As the amount of C in the solid increases, the implanted atoms nucleate to form deposits on the Si surface. The presence of these features significantly decreases the ability of the C_{60}^+ projectile to remove material from the solid. In turn, the rate of C deposition increases or “turns-on”—leading to formation of a large C mound-like structure covering the Si surface [5,6,13].

Decreasing the amount of C deposited at the Si surface during C_{60}^+ erosion is key to avoiding the occurrence of artifacts. The simplest approach for accomplishing this feat involves increasing the number of atoms removed for each C_{60}^+ impact. Sputter yield is known to increase as the amount of energy deposited in the near surface region of the solid increases [14]. One strategy for increasing the amount of energy deposited at the surface is to increase the kinetic energy of the projectile [14]. The result of increasing the C_{60}^+ incident energy from 10 keV to 40 keV at 40° incidence on the bombardment of Si is shown in Fig. 2b. The AFM measurements show the formation of a deep sputter crater within the Si solid. The SIMS images indicate that the bottom of this crater is not covered by a pure C layer but instead consists of a Si and C mixture. These observations suggest 40 keV, 40° incident C_{60}^+ sputtering of Si is characterized by net erosion only and not the occurrence of net deposition. This behavior is attributed to the removal rate being large enough to limit the amount of C accumulated at the Si surface—eliminating the formation of C features which reduce yield and “turn on” deposition. Although this observation is encouraging in terms of depth profiling, the intrinsic surface roughness of the C_{60}^+

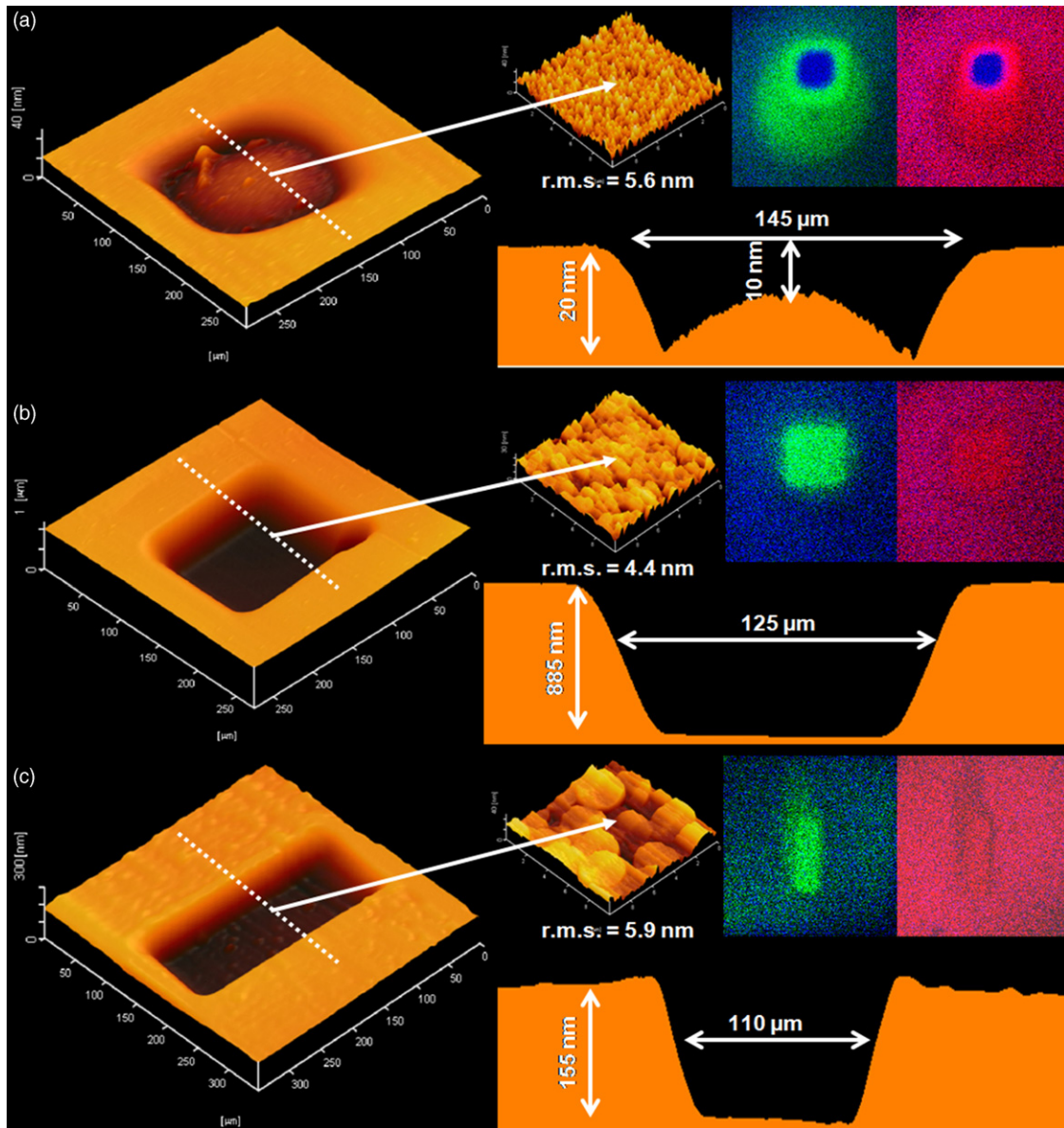


Fig. 2. AFM representations and chemical-specific SIMS images of a Si crystal bombarded with (a) 10 keV, 40° incident C_{60}^+ , (b) 40 keV, 40° incident C_{60}^+ , and (c) 10 keV, 75° incident C_{60}^+ . The field of view for the AFM representations is $\sim 300 \mu\text{m} \times 300 \mu\text{m}$. The solid white arrow indicates the region from which the surface roughness measurement (root-mean-square; r.m.s.) was taken. The dashed white line indicates the plane from which the AFM line profile was taken. The field of view for the molecule-specific SIMS images is $\sim 400 \mu\text{m} \times 400 \mu\text{m}$. The red signal represents the Si intensity (Si_n^+ where $n = 1, 2$; $m/z = 27.98, 55.96$), the blue signal represents the C intensity (C_n^+ where $n = 1, 3, 4, 5, 10, 15$; $m/z = 12.00, 36.00, 48.00, 60.00, 120.00, \text{ and } 180.00$), and the green signal represents the Si–C intensity (Si_nC^+ where $n = 2, 3, 4$; $m/z = 67.96, 95.94, 123.92$). All images were acquired using a focused 40 keV, 40° incident C_{60}^+ ion beam.

bombarded Si surface is 4.4 nm, eliminating the possibility for ultra-high depth resolution.

An additional strategy for increasing the sputter yield and decreasing the amount of C implanted into the Si solid involves varying the incident angle geometry of the C_{60}^+ projectile. MD simulations suggest that as the incident angle of the C_{60}^+ projectile is increased, the energy is deposited closer to the solid surface, with a larger fraction of the energy being reflected back into the vacuum [7,8]. While this behavior results in a lower sputter yield, it may also lead to a smaller altered layer depth and fewer C atoms being implanted into the surface [6–8,13]. The effect of changing the C_{60}^+ incident angle from 40° to 75° at 10 keV is illustrated in Fig. 2c. This result is qualitatively similar to the 40 keV, 40° incident C_{60}^+ experiment and dissimilar to the 10 keV, 40° incident C_{60}^+ experiment. That is, the AFM measurements show a sputter

crater within the Si and no indication of a mound-like structure. Moreover, the SIMS images indicate the crater is characterized by a Si and C mixture and not a pure C layer. These observations suggest glancing incident angles reduce the amount of C accumulated during the C_{60}^+ bombardment of Si. While the results are promising since low energy, glancing incident angles have been demonstrated to improve depth resolution during sample erosion, the roughness of the bombarded surface is 5.9 nm, complicating application to ultra-shallow depth profiling [1,2,5].

4. Conclusions

We have shown that the profile of the energy deposition footprint of the C_{60}^+ bombardment event can be controlled to reduce the formation of artifacts during erosion of Si by increasing

the incident energy and/or increasing the incident angle. At this stage, however, each of the studied parameters results in a topography which is large enough to prevent ultra-shallow depth profiling. The roughening of the surface is attributed to the final chemistry of the bombarded surface, i.e. the incorporation of some C into the Si crystal. Given the strong dependence of the deposition of C on the C_{60}^+ parameters observed to this point, we believe it may be possible to reduce the topography to acceptable levels for ultra-high depth resolution by using even more glancing incident angles, lower kinetic energies, oxygen backfilling, and/or temperature controlled experiments [1,2,5,15].

In addition to semiconductor applications, the research provides fundamental insight into the effect of C_{60}^+ incident geometry on the bombardment of Si. We find that at 10 keV kinetic energy, the sputter yield increases substantially when the incident angle is increased from 40° to 75° . Conversely, at 20 keV and 40 keV kinetic energy, the sputter yield remains practically unchanged when the incident angle is increased. Additionally, yield measurements taken from a molecular solid in a complementary study find that yield decreases when the incident angle is increased from 40° to 73° [7–10]. Hence, it can be concluded that the relative effect of changing the C_{60}^+ incident angle on the profile of the energy deposition footprint, and thus sputter yield, varies according to both the kinetic energy of the projectile and the material of the bombarded surface, a behavior that is quite different than the phenomenon associated with atomic projectile bombardment.

Acknowledgements

The authors acknowledge the National Science Foundation under grant # CHE-555314 and Department of Energy under grant # DE-FG02-06ER15803 for partial financial support of this research. The authors would also like to acknowledge B.J. Garrison for helpful discussions.

References

- [1] A. Zalar, E.W. Seibt, P. Panjan, *Thin Solid Films* 246 (1994) 35–41.
- [2] Y. Kataoka, T. Itani, *Surface and Interface Analysis* 39 (2007) 826–831.
- [3] N. Winograd, *Analytical Chemistry* 77 (2005) 142A–149A.
- [4] Z. Postawa, B. Czerwinski, M. Szweczyk, E.J. Smiley, N. Winograd, B.J. Garrison, *Journal of Physical Chemistry B* 108 (2004) 7831–7838.
- [5] G. Gillen, J. Batteas, C.A. Michaels, P. Chi, J. Small, E. Windsor, A. Fahey, J. Verkouteren, K.J. Kim, *Applied Surface Science* 252 (2006) 6521–6525.
- [6] K.D. Krantzman, D.B. Kingsbury, B.J. Garrison, *Applied Surface Science* 252 (2006) 6463–6465.
- [7] K.E. Ryan, E.J. Smiley, N. Winograd, B.J. Garrison, *Applied Surface Science*, in press.
- [8] K.E. Ryan, B.J. Garrison, *Analytical Chemistry*, in press.
- [9] J. Kozole, D. Willingham, N. Winograd, *Applied Surface Science*, in press.
- [10] J. Kozole, A. Wucher, N. Winograd, *Analytical Chemistry*, in press.
- [11] R.M. Braun, P. Blenkinsopp, S.J. Mullock, C. Corlett, K.F. Willey, J.C. Vickerman, N. Winograd, *Rapid Communications in Mass Spectrometry* 12 (1998) 1246–1252.
- [12] D. Weibel, S. Wong, N. Lockyer, P. Blenkinsopp, R. Hill, J. Vickerman, *Analytical Chemistry* 75 (2003) 1754–1764.
- [13] K.D. Krantzman, R.P. Webb, B.J. Garrison, *Applied Surface Science*, in press.
- [14] M.F. Russo, C. Szakal, J. Kozole, N. Winograd, B.J. Garrison, *Analytical Chemistry* 79 (2007) 4493–4498.
- [15] L. Zheng, A. Wucher, N. Winograd, *Applied Surface Science*, in press.